fractalRegression: An R package for multiscale regression and fractal analyses

Aaron D. Likens[1] & Travis J. Wiltshire[2]

[1] Department of Biomechanics, University of Nebraska at Omaha

[2] Department of Cognitive Science & Artificial Intelligence, Tilburg University

Author Note

Add complete departmental affiliations for each author here. Each new line herein must be indented, like this line. Enter author note here.

The authors made the following contributions. Aaron D. Likens: Conceptualization, Software, Writing - Original Draft Preparation, Writing - Review & Editing; Travis J. Wiltshire: Writing - Original Draft Preparation, Writing - Review & Editing, Software.

Correspondence concerning this article should be addressed to Aaron D. Likens, Postal address. E-mail: alikens@unomaha.edu

Abstract

Time series data from scientific fields as diverse as astrophysics, economics, human movement science, and neuroscience all exhibit fractal properties. That is, these time series often exhibit self-similarity and long-range correlations. This `fractalRegression` package implements a number of univariate and bivariate time series tools appropriate for analyzing noisy data exhibiting these properties. These methods, especially the bivariate tools (Kristoufek, 2015a; Likens, Amazeen, West, & Gibbons, 2019a) have yet to be implemented in an open source and complete package for the R Statistical Software environment. As both practitioners and developers of these methods, we expect these tools will be of interest to a wide audience of scientists who use R, especially those from fields such as the human movement, cognitive, and other behavioral sciences. The algorithms have been developed in C++ using the popular Rcpp (Eddelbuettel & Francois, 2011) and RcppArmadillo (Eddelbuettel & Sanderson, 2014) packages. The result is a collection of efficient functions that perform well even on long time series (e.g., $\geq$ 10,000 data points). In this work, we introduce the package, each of the functions, and give examples of their use as well as issues to consider to correctly use these methods.

Keywords: long range correlation, fractal, multiscale, dynamics

Word count: X

fractalRegression: An R package for multiscale regression and fractal analyses

Introduction

Over time, many signals from living and complex systems exhibit systematic regularities and dependencies across spatial and temporal scales (**kello2010?**). These regularities often follow a power-law (i.e., self-similarity across scales) that are estimated using fractal analyses. Fractal analysis, in its many forms, has become an important framework in virtually every area of science, often serving as an indicator of system health (Goldberger et al., 2002), adaptability (Bak, Tang, & Wiesenfeld, 1987), control (Likens, Fine, Amazeen, & Amazeen, 2015), cognitive function (Euler, Wiltshire, Niermeyer, & Butner, 2016), and multi-scale interactions (Kelty-Stephen, 2017).

In particular, various methods related to Detrended Fluctuation Analysis (DFA) (Peng et al., 1994) have rose to prominence due to their relative ease of understanding and broad applicability to stationary and non-stationary time series, alike. More specifically, in areas of the social and cognitive sciences, DFA, or variants of DFA, have been used to study, for example, reaction times (Van Orden, Holden, & Turvey, 2003), eye gaze (Stephen, Boncoddo, Magnuson, & Dixon, 2009), gait (**delignières2009?**), limb movements (Delignières, Torre, & Lemoine, 2008), heart rate (Goldberger et al., 2002), and neurophysiological oscillations Euler et al. (2016). And, beyond an individual level, the methods have been used to study human-machine system interaction (Likens et al., 2015), tool use (**favela2021?**), and interpersonal coordination in a variety of modalities Delignières, Almurad, Roume, & Marmelat (2016).

Thus, there is a broad scientific appeal for these fractal-based analyses. While, the basic DFA algorithm has been implemented in numerous packages and software programs, more advanced methods such as Multifractal Detrended Fluctuation Analysis (MFDFA) (Kantelhardt et al., 2002), Detrended Cross Correlation Analysis (DCCA) (Podobnik & Stanley, 2008; Zebende, 2011), and, in particular, fractal regression techniques such as

Multiscale Regression Analysis (MRA) (Kristoufek, 2015a; Likens et al., 2019a) have not yet been implemented in a comprehensive software package. A key aspect of this effort is to draw more attention and make more available these *fractal regression* techniques. In particular, we find these methods widely promising because they allow for uncovering "the time scales most relevant to relationships between a system's components" (p. 2) within a predictive framework (Likens et al., 2019a).

Thus, there is a clear need for a package that incorporates this functionality in order to advance theoretical research focused on understanding the time varying properties of natural phenomena and applied research that uses those insights in important and diverse areas such as healthcare (Cavanaugh, Kelty-Stephen, & Stergiou, 2017) and education (Snow, Likens, Allen, & McNamara, 2016). In this work, we provide an overview of our `fractalRegression` package, provide simulated and empirical examples of it's functions, and provide practical advice on the successful application of these methods.

Package Overview

Our `fractalRegression` package for R (Team, 2018) is built on a C++ architecture and includes a variety of uni- and bivariate fractal methods as well as functions for simulating data with known fractional properties (e.g., scaling, dependence, etc.), and surrogate testing. Some foundational efforts in fractal analyses, which partially overlap with the functionality of this package, have been implemented elsewhere. For example, a number of univariate fractal and multifractal analyses have been implemented in the 'fracLab' library for MATLAB (Legrand & Véhel, 2003) and other toolboxes that are mainly targeted at multifractal analysis (E. A. F. Ihlen, 2012; Espen A. F. Ihlen & Vereijken, 2010). In terms of open access packages, there are other packages that implement some, but not all of the same functions such as the `fathon` package (Bianchi, 2020) that has been implemented in Python as well as the R packages: `fractal` [defunct], `nonlinearTseries` (Garcia, 2020), and `MFDFA` (Laib, Golay, Telesca, & Kanevski, 2018).

However, none of the above packages incorporate univariate monofractal and multifractal DFA with bivariate DCCA and MRA and some are only written in less efficient base R code. Our `fractalRegression` package is unique in this combination of analyses and efficiency (particularly for long time series). For instance, we are not aware of any other packages that feature MRA. In addition, we expect that featuring simulation methods as well as surrogate testing strongly bolsters the accessibility of these methods for the social and cognitive science community in particular, but also science, more generally.

Methodological Details and Examples

In order to demonstrate the methods within the 'fractalRegression' package, we group this into univariate (DFA, MFDFA) and bivariate methods (DCCA, MRA). For each method, we 1) highlight the key question(s) that can be answered with that method, 2) briefly describe the algorithm with references to additional details, 3) describe some key considerations for appropriately applying the algorithm, and demonstrate the use of the functions on a 4) simulated and 5) empirical application of the function. An overview of the core functions included in the package, the general objective of that function, and the output are shown below in Table 1. Note that there are some additional helper and plotting functions included as well. The additional details are included in the sections corresponding to those methods, in the package documentation, and in the original sources for the methods.

Table 1.

Overview of core package functions, objectives, and output

Univariate Methods

Detrended Fluctuation Analysis. A key question that can be answered by Detrended Fluctuation Analysis (DFA) (Peng et al., 1994) is: *what is the magnitude and* *direction of long range correlation in a single time series?* While DFA has been described extensively elsewhere (Kantelhardt, Koscielny-Bunde, Rego, Havlin, & Bunde, 2001) and visualized nicely (Kelty-Stephen et al., 2016), we provide a brief summary here. DFA entails splitting a time series into several small bins (e.g., 16). In each bin, a least squares regression is fit and subtracted within each window. Residuals are squared and averaged within each window. Then, the square root is taken of the average squared residual across all windows of a given size. This process repeats for larger window sizes, growing by, say a power of 2, up to N/4, where N is the length of the series. In a final step, the logarithm of those scaled root mean squared residuals (i.e., fluctuations) is regressed on the logarithm of window sizes. The slope of this line is termed α and it provides a measure of the long range correlation. α is commonly used an as estimator of the Hurst exponent (H), where $\alpha < 1 = H$, and for $\alpha > 1$, $H = 1 - \alpha$. Conventional interpretation of α is: $\alpha < 0.5$ is anti-correlated, $\alpha\ = 0.5$ is uncorrelated, white noise, $\alpha > 0.5$ is temporally correlated, $\alpha\ = 1$ is long-range correlated, 1/f-noise, pink noise, $\alpha > 1$ is non-stationary where the special case $\alpha\ = 1.5$ is fractional Brownian noise. More generally, $1 < \alpha < 2$ are referred to as fractional Brownian motion.

DFA Examples. To demonstrate the use of `dfa()` we simulate three time series using the `fgn_sim()` function. This is a simple function based on the former `fARMA` R package. It requires the number of observations `n`, and the Hurst exponent `H`. In particular, we simulate white noise, pink noise, and anti-correlated fractional Gaussian noise using the code below.

```
white.noise <- fgn_sim(5000, H = 0.5)

pink.noise <- fgn_sim(n = 5000, H = 0.9)

anti.corr.noise <- fgn_sim(5000, H = 0.25)
```

```
scales <- logscale(scale_min = 16, scale_max = 1024, scale_ratio = 2)
```

Then, we run DFA on those simulated series using the example code below. Note that this example uses linear detrending with minimum scale of 16, a maximum scale that is at most 1/4 the time series length, and scale factor (`scale_ratio`) of 2, which is evenly spaced in the logarithmic domain (see General Discussion for more details and considerations for these parameter choices).

```
dfa.white <- dfa(x = white.noise, order = 1, verbose = 1, scales=scales, scale_ratio = 2

dfa.pink <- dfa(x = pink.noise, order = 1, verbose = 1,
scales=scales, scale_ratio = 2)

dfa.anti.corr <- dfa(x = anti.corr.noise, order = 1, verbose = 1, scales=scales, scale_r
```

In terms of output from the above examples, for white noise, we observed that $\alpha =$ 0.50, for pink noise we observed that $\alpha = 0.82$, and since we simulated anti-correlated noise with H = 0.25, we observed a close estimate of the $\alpha = 0.24$. In terms of the objects saved from the `dfa()` function, one commonly inspects the log(scales)-log(fluctuation) plots. Given the estimates above, we see in Figure 1 that the slopes for white noise, pink noise, and anti-correlated noise conform to our expectations. These slope estimates (and R^2) are provided n the equation listed above each respective line, and are generated using the `dfa.plot()` function.

Figure 1

Log scale-Log fluctuation plots for white noise (top), pink noise (middle), and anti-correlated noise (bottom)

```
par(mfrow=c(1,3))
dfa.plot(dfa.white)
dfa.plot(dfa.pink)
dfa.plot(dfa.anti.corr)
```

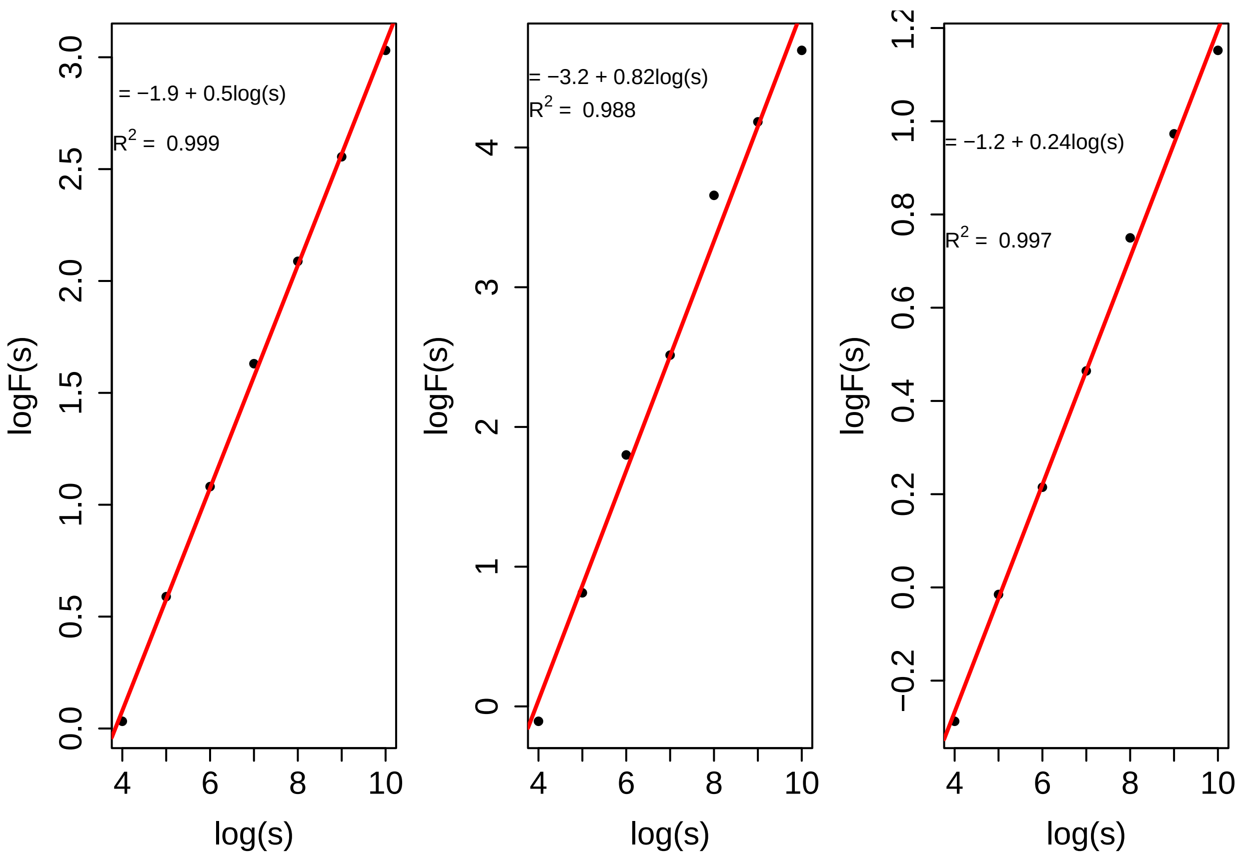

For an empirical example, we apply the `dfa()` function to the Human Balance Dataset (Santos & Duarte, 2016). This publicly available dataset includes signals from a force platform that measures the center of pressure in the x and y dimensions for 87 young adults (we exclude the older adults from our analyses for simplicity). Trials lasted 60s. See original paper for additional details on data processing (Santos & Duarte, 2016). For the empirical examples, we use two different time series featuring a participant standing on a firm (rigid) surface with eyes open and a foam (unstable) surface with eyes open. We chose this dataset because postural sway data are known to exhibit interesting fractal dynamics

(Collins & De Luca, 1993; Delignières, Torre, & Bernard, 2011a; Delignières, Torre, & Bernard, 2011b) and we can systematically evaluate the data for all of the univariate and bivariate analyses included in the package.

For center of pressure (COP) data, we take the first order differences of each series using the `diff()` function as a rough approximation of COP velocity. For the univariate analyses, we focus on analyses of the COP data in the x dimension. Then, we define the appropriate scales for the analyses using the same methods shown above, except we use a `scale ratio = 1.1` for a higher density of points. Figure 2 shows the results of these analyses.

Figure 2

Log scale-Log fluctuation plots for empirical differenced COPx time series for rigid/firm (left) and unstable/foam (right) surfaces.

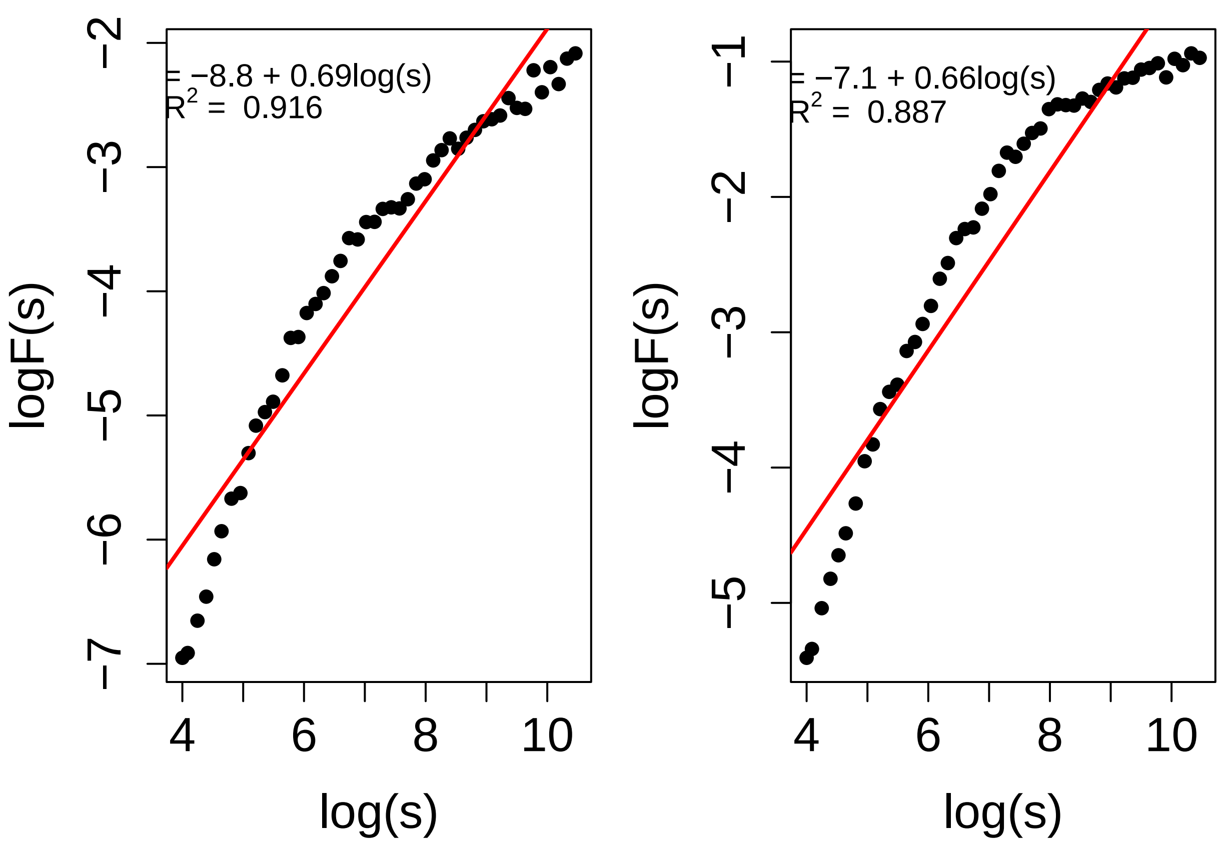

Importantly, regarding the question one can ask using DFA, we observe from Figure 2, that long range correlations are positive and approximately 0.69 - 0.66. However, from visual inspection of these plots we observe that two slopes might fit better than one for these time series; a phenomenon known as crossover points (Collins & De Luca, 1993; Ge & Leung, 2013). One common approach when such crossover points exist is to recognize that the signal might be best characterized by two scaling regions, before and after an inflection point. We provide an example of how to check for where the break point is below using piece-wise regression .

Figure 3

Log scale-Log fluctuation plots for empirical differenced COPx time series for rigid/firm surfaces with lines plotted for piece-wise regression slopes

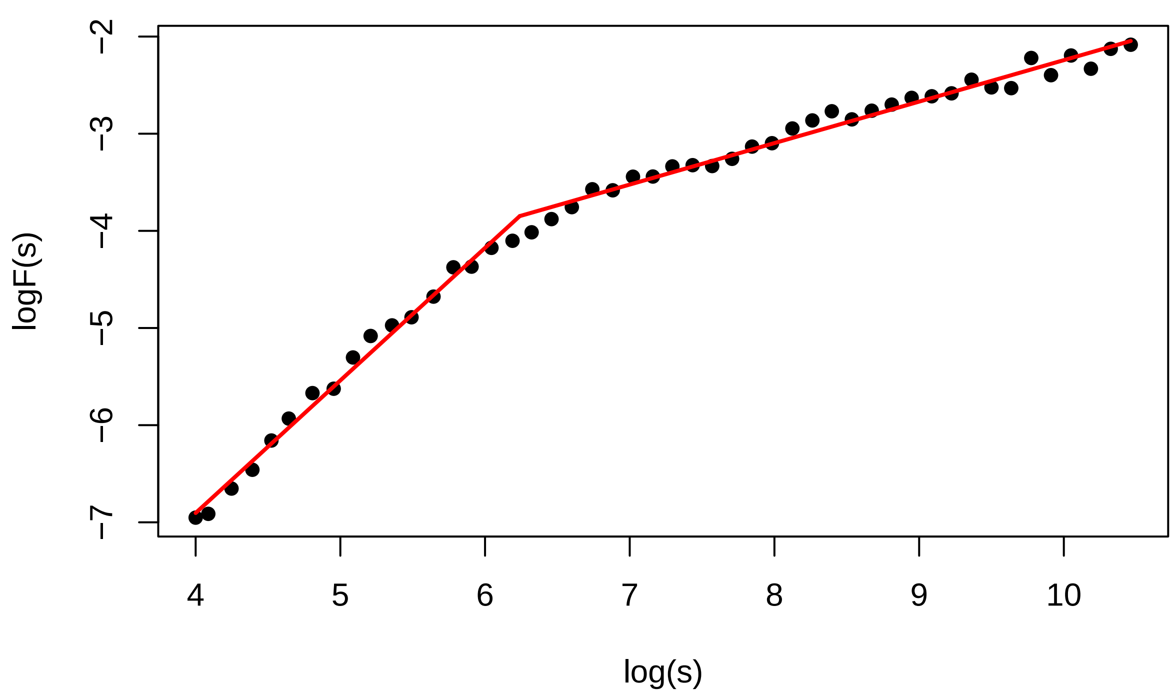

In the example above, we observe a crossover point at around the scale size of log 6. And, from the results in Table 2 below, we observe that there are two distinct scaling relationships corresponding to $\alpha = 1.3$ and $\alpha = 0.42$, respectively. This is a well known result in the postural control literature such that short time scales correspond to persistent temporal correlation and the longer time scales correspond to anti-persistent correlation. More substantively, short time scale dynamics correspond to periods of exploratory sway, whereas longer time scales correspond to corrective movements that prevent exceeding the base of support and falling (Collins & De Luca, 1993; Delignières et al., 2011a; Delignières et al., 2011b).

Table 2

Results from piece-wise-regression analysis

Multifractal Detrended Fluctuation Analysis. Multifractal Detrended Fluctuation Analysis (MFDFA; Kantelhardt et al. (2002)) is an extension of DFA by generalizing the fluctuation function to a range of exponents of the qth order. The key question that can be answered by MFDFA is: *how does the magnitude and direction of long range correlation change over time within a single time series?* Like DFA, MFDFA entails splitting a time series into several small bins (e.g., 16). In each bin, least squares regression is fit and subtracted within each window. However, the residuals are raised to a range of exponents q and averaged within each window. So when $q = 2$, MFDFA reduces to ordinary DFA. When $q > 2$, relatively larger residuals are emphasized and when $q < 2$, relatively smaller residuals are emphasized. The rest of the DFA algorithm is performed for each window and windows size for all values of q. We refer the reader to the work of Kelty-Stephens and colleagues Kelty-Stephen et al. (2016) . Figure 3 for a visualization of the algorithm and to Kantelhardt and colleagues Kantelhardt et al. (2002) for additional mathematical description.

MFDFA Examples. To demonstrate the use of `mfdfa()`, we work with data included in our package (`fractaldata`), that was originally provided by E. A. F. Ihlen (2012). It includes a white noise time series, a monofractal time series, and a multifractal time series. These data are shown below in Figure 4.

Figure 4

Time series from Ihlen (2012) corresponding to white noise, monofractal, and multifractal series

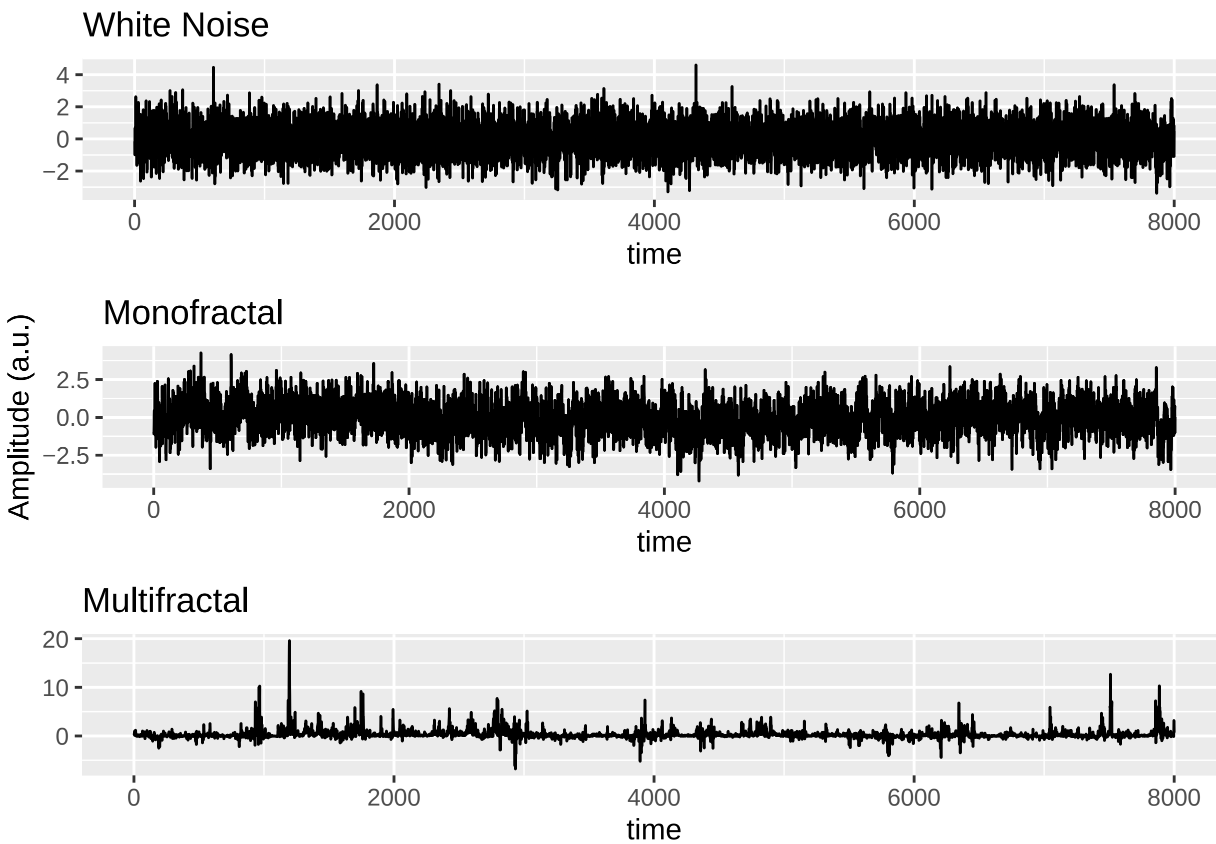

Performing MFDFA is straight forward with the `mfdfa()` function. As shown in the example below, one enters the time series `x` to perform the analysis on, the range of `q` order exponents to use, the `order` of polynomial detrending, and the `scales` for the analysis. In this case, we define our `scales` by choosing logarithmically spaced scales and we select values of q from -5 to 5. Note here that the scale factor need not be a power of two but should be evenly spaced in the logarithmic domain by, for example, using different logarithm bases. We provide the `logscale()` function to facilitate scale construction.

```
scales <- logscale(scale_min = 16,scale_max = 1024,scale_ratio = 1.1)

white.mf.dfa.out <- mfdfa(x = fractaldata$whitenoise, q = c(-5:5), order = 1, scales=sca

mono.mf.dfa.out <- mfdfa(x = fractaldata$monofractal, q = c(-5:5), order = 1,  scales=sc

multi.mf.dfa.out <- mfdfa(x = fractaldata$multifractal, q = c(-5:5), order = 1,  scales=
```

A common way to understand if there is evidence of multifractality is to examine a plot showing the slopes of the `log_fq` at the `log_scale` values. If all the plots have the same slope, that provides evidence of monofractality. If there are distinct slopes, then there is evidence of multifractality. It's also important to check here that the slopes of `log_scale` and `log_fq` are approximately linear, thus implying that they are scale invariant. If not, then it could be the case that a higher order polynomial detrending is appropriate (see Kantelhardt et al., 2001). Figure 5 shows what we would expect for a monofractal and multifractal signal. In other words, the monofractal signal shows a consistent slope, whereas the multifractal signal shows variability in the slopes. Importantly, Figure 5, using our `mfdfa.plot()` function shows various aspects of mfdfa for each value of q (each with its own color) includes panels that show the log(scale)-log(Fluctuation) plots like in the DFA plots (top left), the slopes of those lines as the q-order Hurst exponents ($H(q)$ for each value of q (top right), the mass exponents ($\tau(q)$) for each value of q (bottom left), and the multifractal spectrum showing q-order singularity values (h) for their dimension (D(h) for each value of q (bottom right). See Ihlen (2012) for additional details of these metrics.

Figure 5

Mfdfa.plots for mono-(top) and multifractal series (bottom)

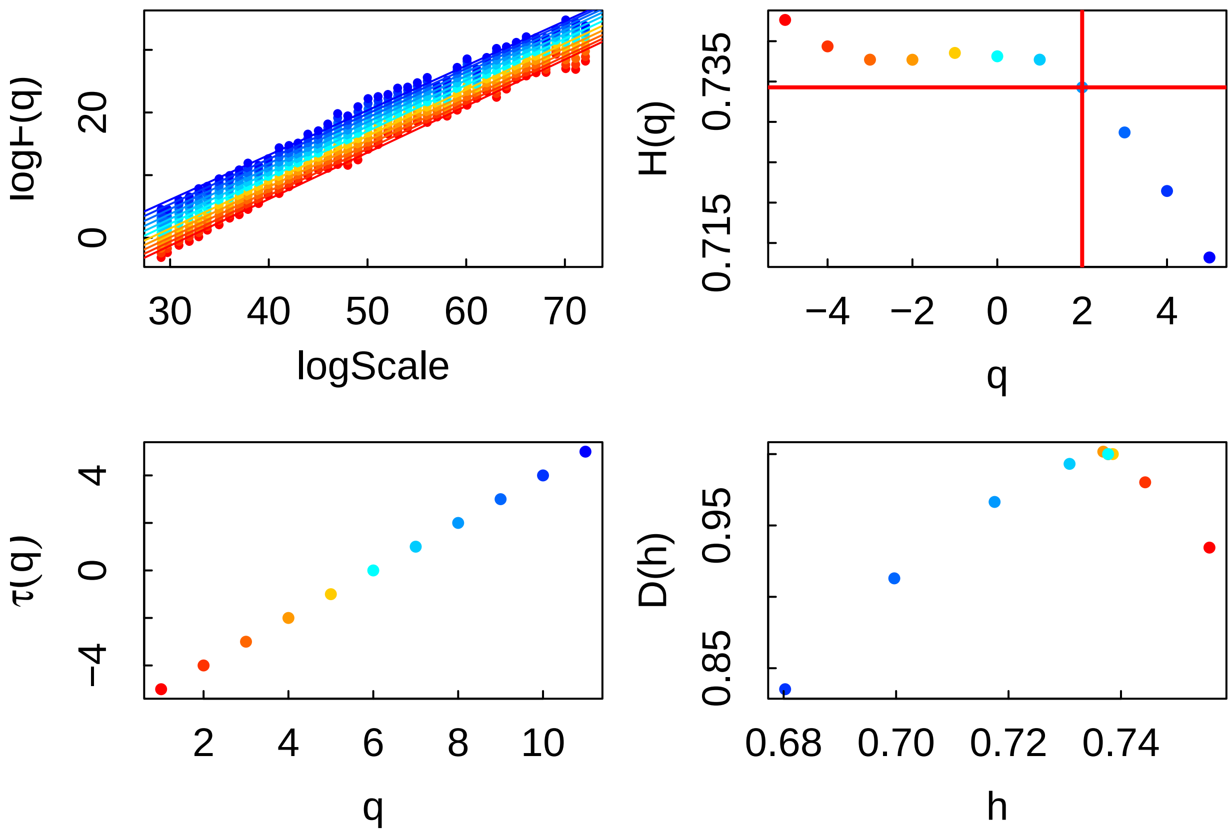
logF(q)
0
20
30
40
50
60
70
logScale
H(q)
0.715
0.735
−4
−2
0
2
4
q
τ(q)
−4
0
4
2
4
6
8
10
q
D(h)
0.85
0.95
0.68
0.70
0.72
0.74
h

235

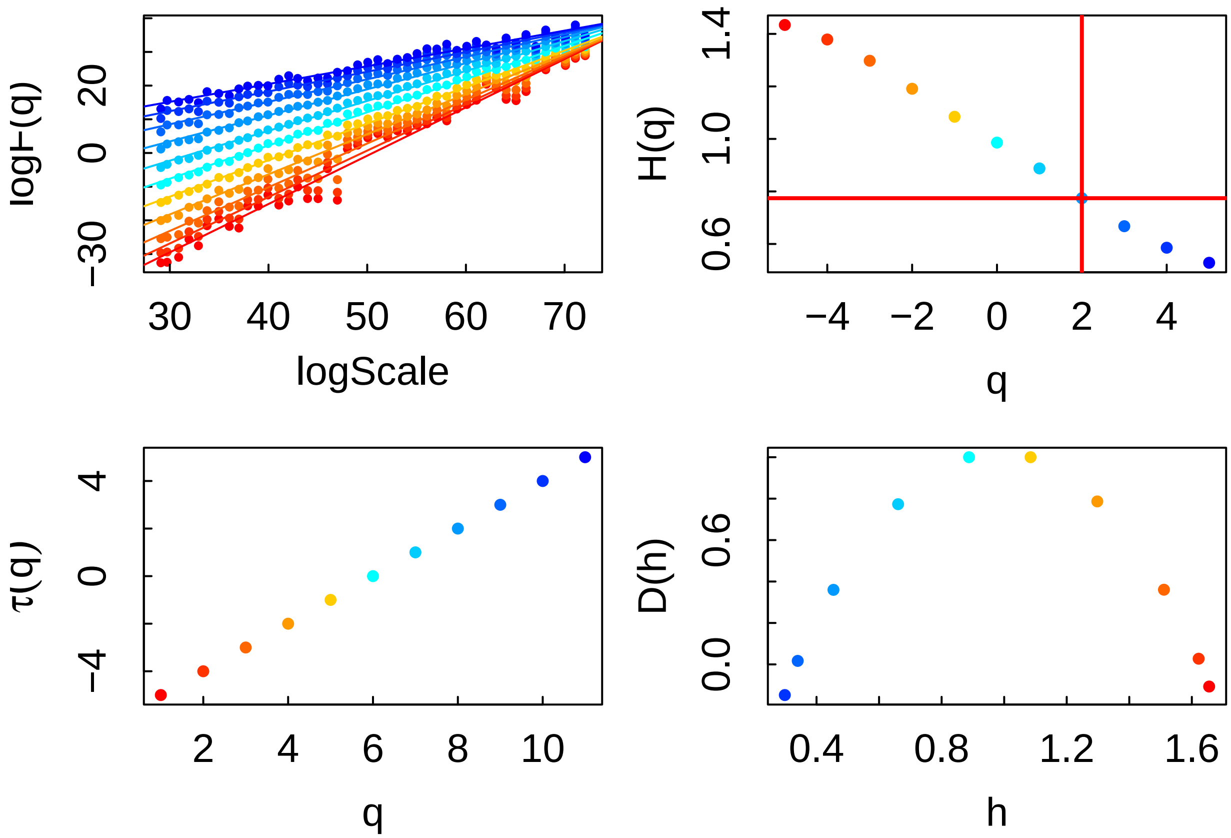

A common metric for comparing multifractal spectra is to calculate the width (W) as $h_{max} - h_{min}$. Let's do this to compare the monofractal and multifractal time series. We observe in this case that for the monofractal signal $W_{mono} = 0.08$ and $W_{multi} = 1.36$. If we compare the spectra for the mono- and multifractal signals above (bottom right of both plots), we observe this clear difference in the widths of the multifractal spectra for the signals.

For our empirical analysis, we again turn to the postural data. We set our parameters appropriate for the data and run `mfdfa()` on the differenced COPx data for the firm and foam surfaces. Figure 6 shows the plots for these analyses. In particular, we observe for both surfaces that the q-order Hurst exponents range from 0.57 - 1.03, all suggesting positive long-range correlations with a weakening of the strength at larger values of q (i.e., trending towards white noise). The multifractal spectrum widths of the two surfaces were also similar, $W_{foam} = 0.69$ and $W_{firm} = 0.70$.

Figure 6

Mfdfa.plots for the firm (top) and foam surfaces (bottom)

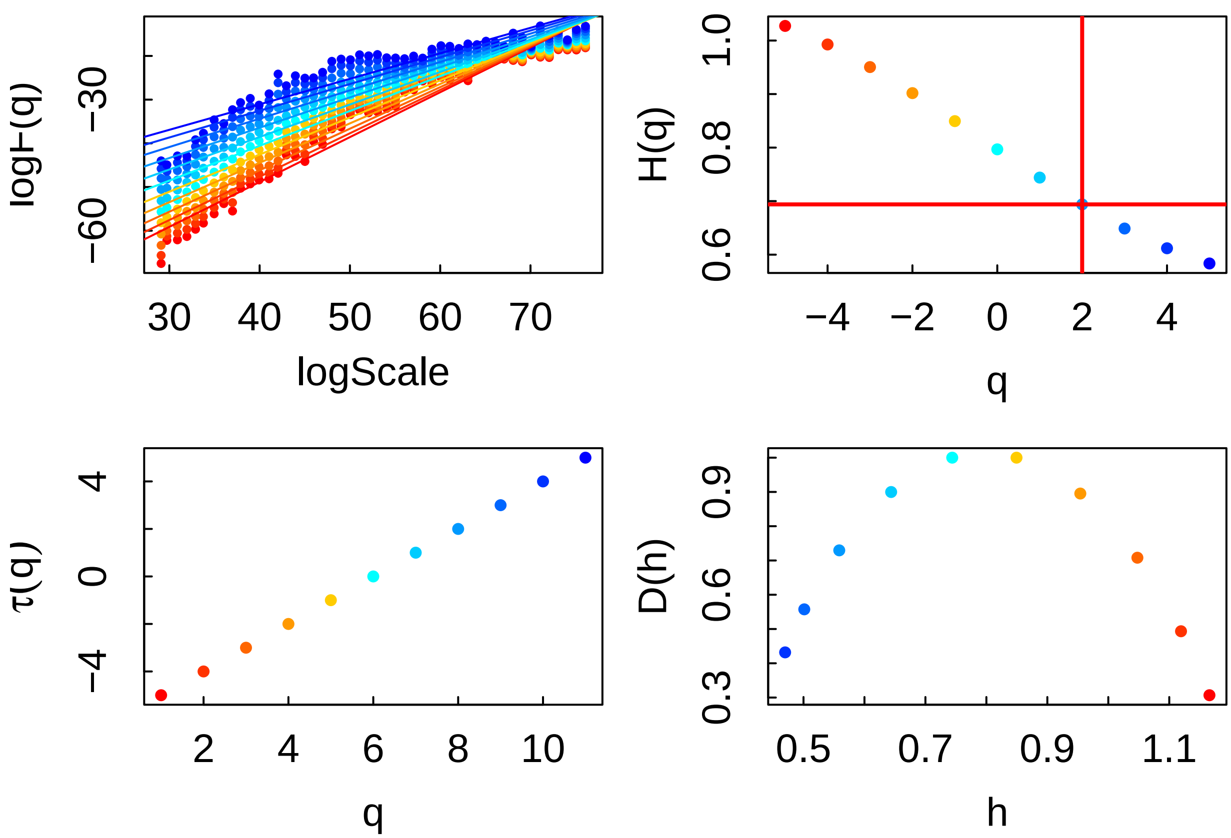

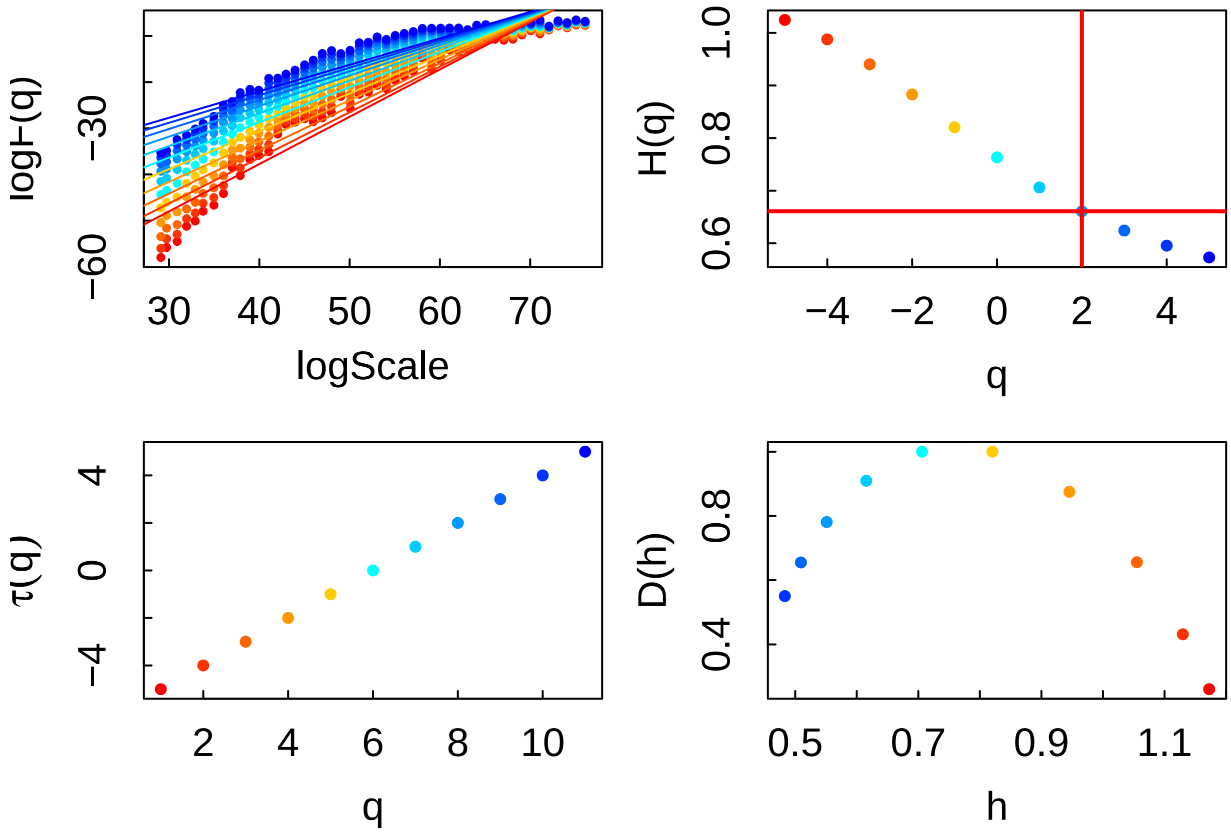

Bivariate Methods

Detrended Cross-Correlation Analysis. Detrended Cross-Correlation Analysis (DCCA; Podobnik and Stanley (2008), Zebende (2011)) is a bivariate extension of the DFA algorithm generalizing it to a correlational case between two time series that may be non-stationary. The key questions that can be asked with it are: a) *How does correlation between two time series change as a function of scale?* and b) *What is/are the dominant (time) scale(s) of coordination?* Such decisions are based on a predetermined threshold such as a conventional statistical significance as we demonstrate below. Researchers may also select other criteria appropriate for their research area.The DCCA algorithm is a direct generalization of the DFA algorithm but applied to two concomitantly measured time series, say x and y. As in DFA, time series are split into multiple bins and detrended using least squares regression. Separate regressions are performed for x and y. Within each bin, three quantities are estimated, the average squared residual of x, the average squared residual of y, and the average cross product (i.e., the covariance) between the residuals for x and the residuals for y. Each of those quantities is averaged across all bins of a given size. After taking the squared residual for x and y, we obtain scale-wise equivalents of covariance $F_{xy}(s)$ and standard deviations for x $F_x(s)$ and y $F_y(s)$. The use of F to designate these quantities derives from originating literature(Kristoufek, 2015b; Likens, Amazeen, West, & Gibbons, 2019b). Thus, the scale-wise regression coefficient, the estimand of DCCA, is the following quotient:

$$\rho(s) = \frac{F_{xy}(s)}{F_x(s)F_y(s)}$$

Simplified, with DFA, the key metric is α, but in DCCA, one estimates the scale-specific, detrended cross-correlation coefficient $\rho(s)$ for the pair of time series.

DCCA Examples. To demonstrate the use of `dcca()`, we used the `mc_arfima()` function from our package to simulate two time series with known properties. Specifically, we use the multicorrelated ARFIMA examples from Kristoufek's work (Kristoufek, 2013). In this case, we use the parameters from Kristoufek (2013) for Model 1 (p. 6,487), that generates two time series of length 10,000 that exhibit long range correlations (LRC) as well as long range cross-correlations (LRCC). The code for simulating these two time series is shown below. Additionally, Figure 7, shown below, visualizes a subset of these time series.

Figure 7

Subset of two time series exhibiting long range correlation and long range cross-correlation

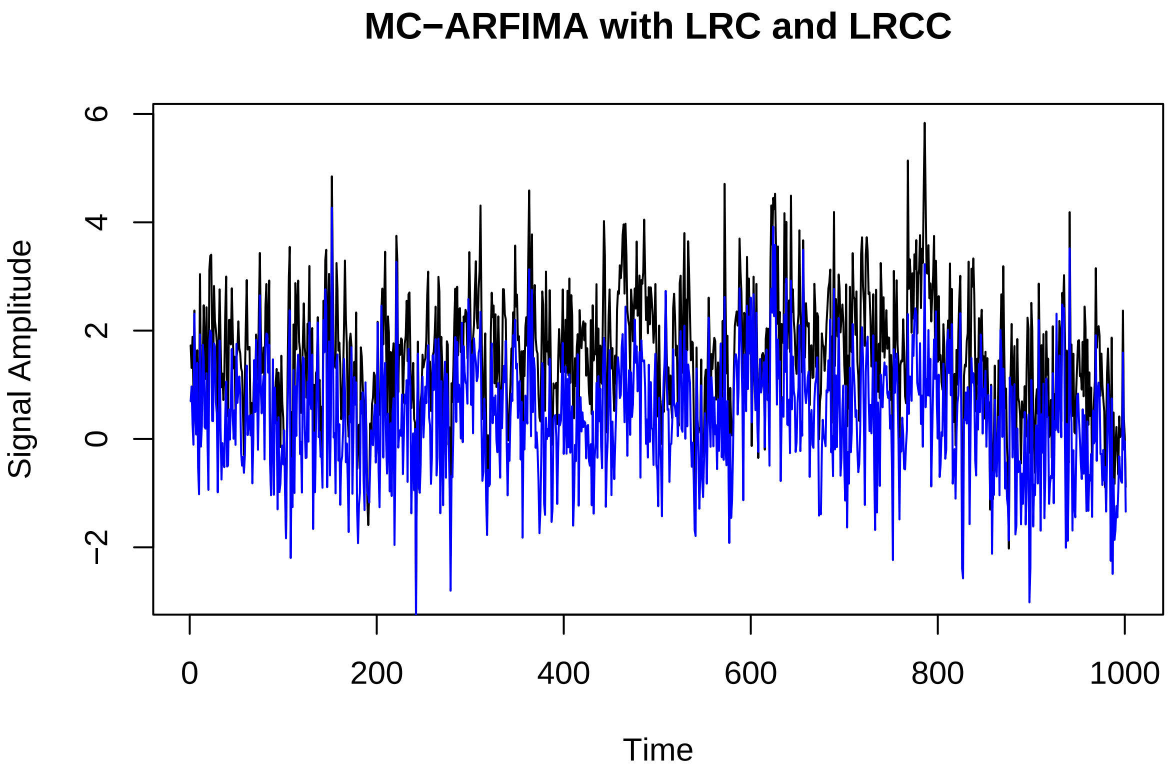

As can be seen in Figure 7, the simulated time series, although quite noisy, appear to covary over time with similar trends. To perform the `dcca()` on these time series, we use the code below, where we first define the `scales` using the `logscale()` function described earlier along with the `dcca()` function itself.

Next, we visualize the output of DCCA in Figure 8. We observe that, as expected, the correlation between the MC-ARFIMA processes are consistently high (all ρ's $> .8$) and continue to be high at increasing time scales.

Figure 8

DCCA output for long range correlation and long range cross-correlation

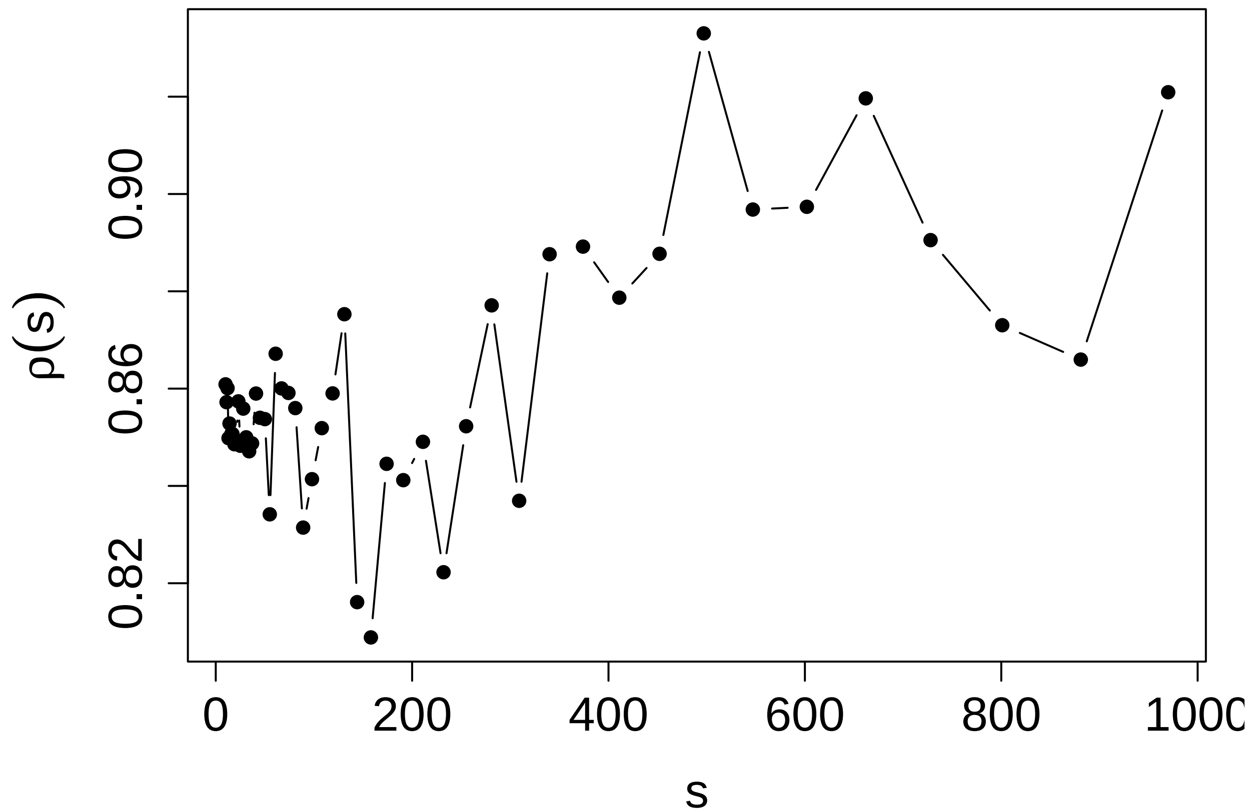

Figure 8 is difficult to interpret on its own. Next we demonstrate an additional plot and analysis feature of `dcca()` by modifying the above code as shown below `ci = TRUE`. Loess smoothing can also be applied to both $\rho(s)$ and its confidence intervals using `loess.rho = TRUE` and `loess.ci = TRUE`. Those latter options are useful for reducing the impact of increasing variance in estimates of $\rho(s)$ at large scales (Likens et al., 2019b). Note though that a much larger set of calculations takes place and may take several seconds up to several minutes (for long time series) to complete.

Figure 9

DCCA output for long range correlation and long range cross-correlation with Loess smoothing on estimates and a surrogate confidence interval

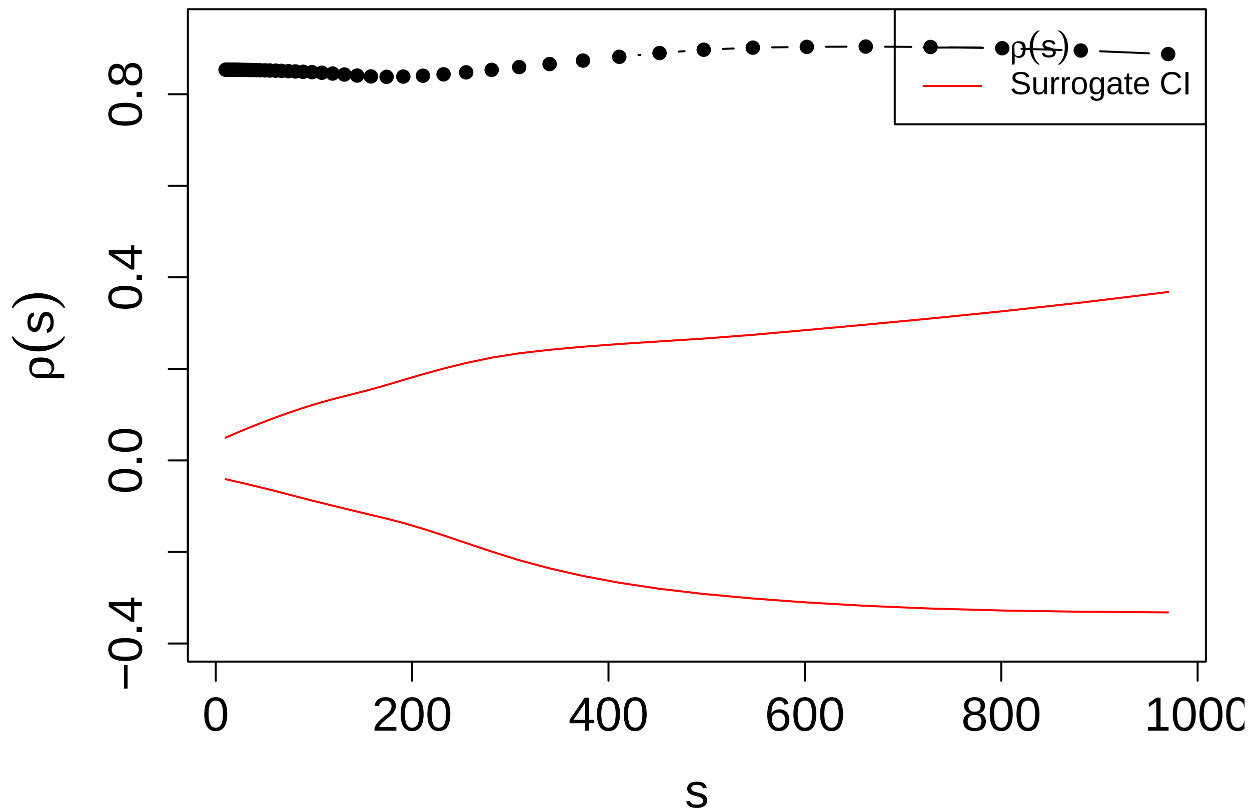

As a point of comparison, we can generate a time series in contrast with this that exhibits processes with LRC and short-range cross-correlation (SRCC) using the code below. In contrast to the previous DCCA analysis, Figure 10 shows a signal that begins with a high cross-correlation (ρ's $\approx .6$) , but that begins to deviate and trend substantially lower at increasing scale sizes with ρ entering the confidence interval containing 0. In fact, based on the plotted confidence intervals, the correlation between the two series becomes non-significant from a conventional standpoint.

Figure 10

DCCA output for long range correlation and short range cross-correlation including smoothing and a surrogate confidence interval

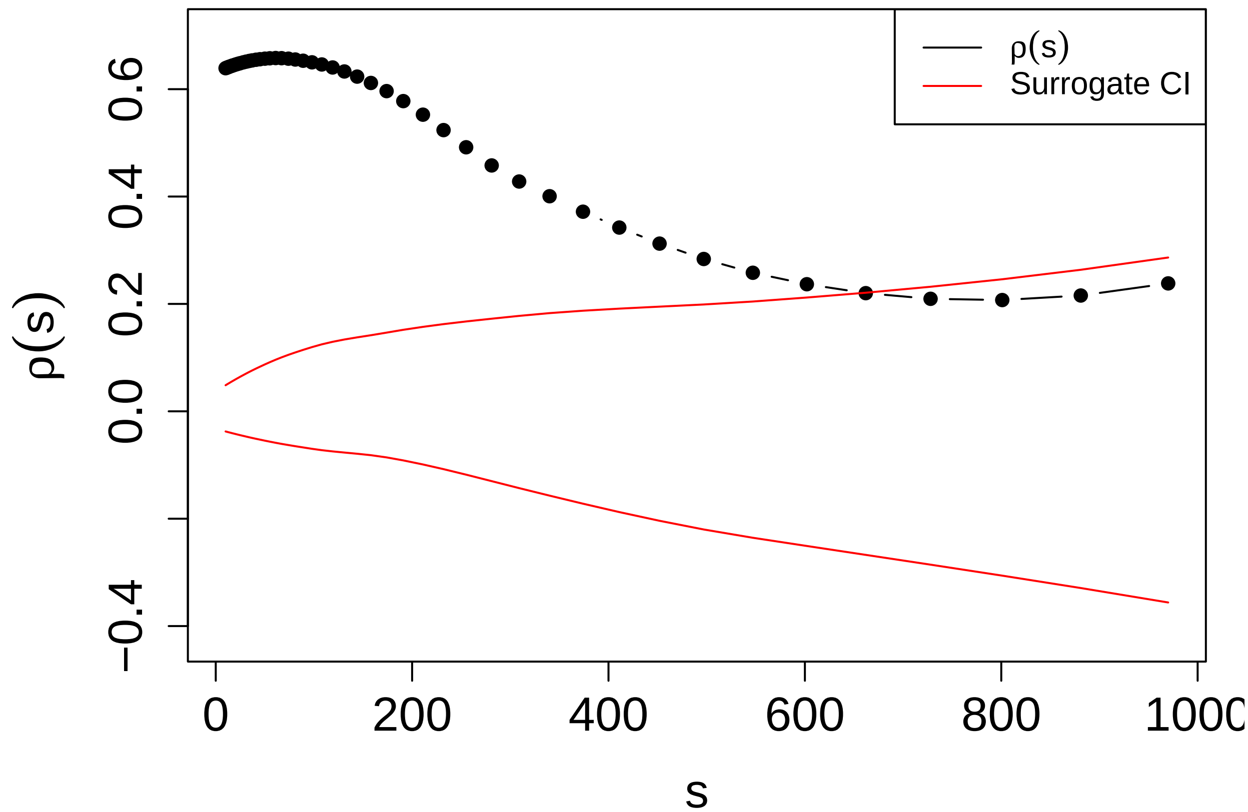

Turning next to the empirical balance data, we apply DCCA to the differenced COPx *and* COPy data for the firm and foam platforms. We again set appropriate values for `scales` and apply the `dcca()` function to the pair of time series.

Figure 11

DCCA output for empirical COPx and COPy balance data for the eyes open while standing on the firm surface (top) and foam surface (bottom)

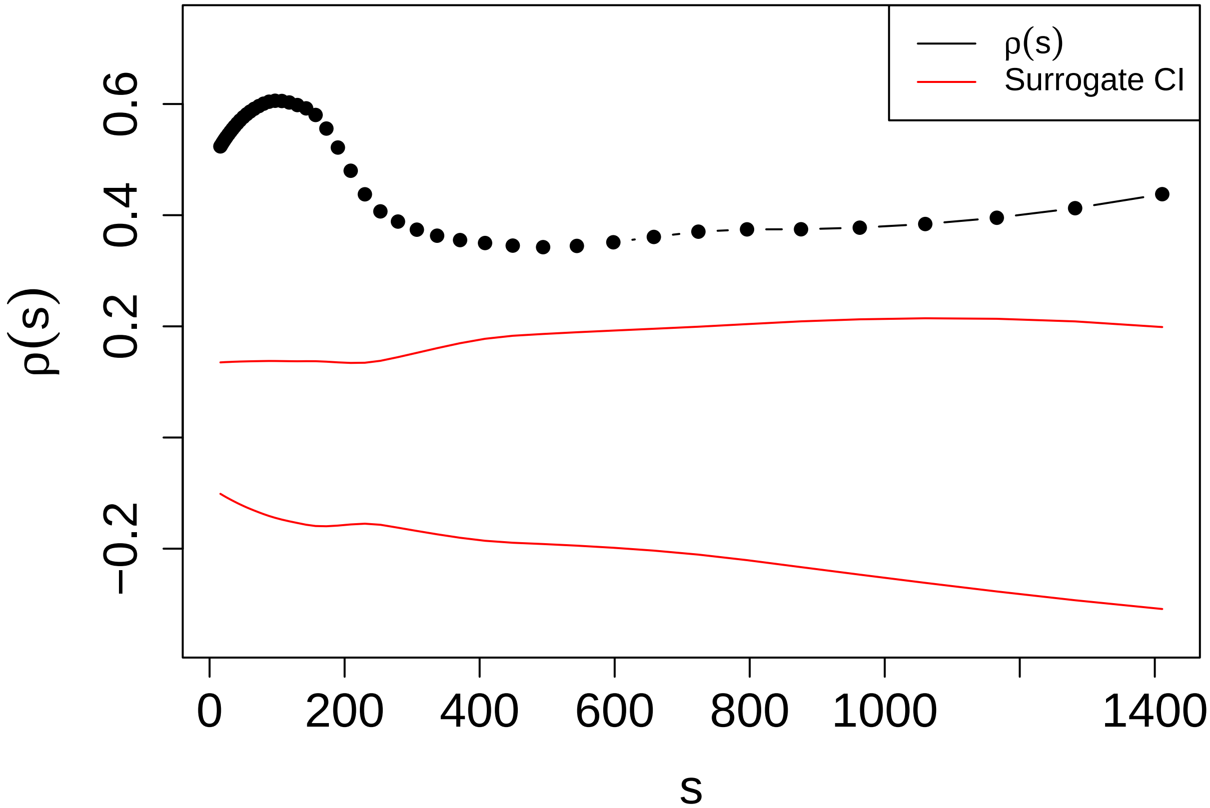

325

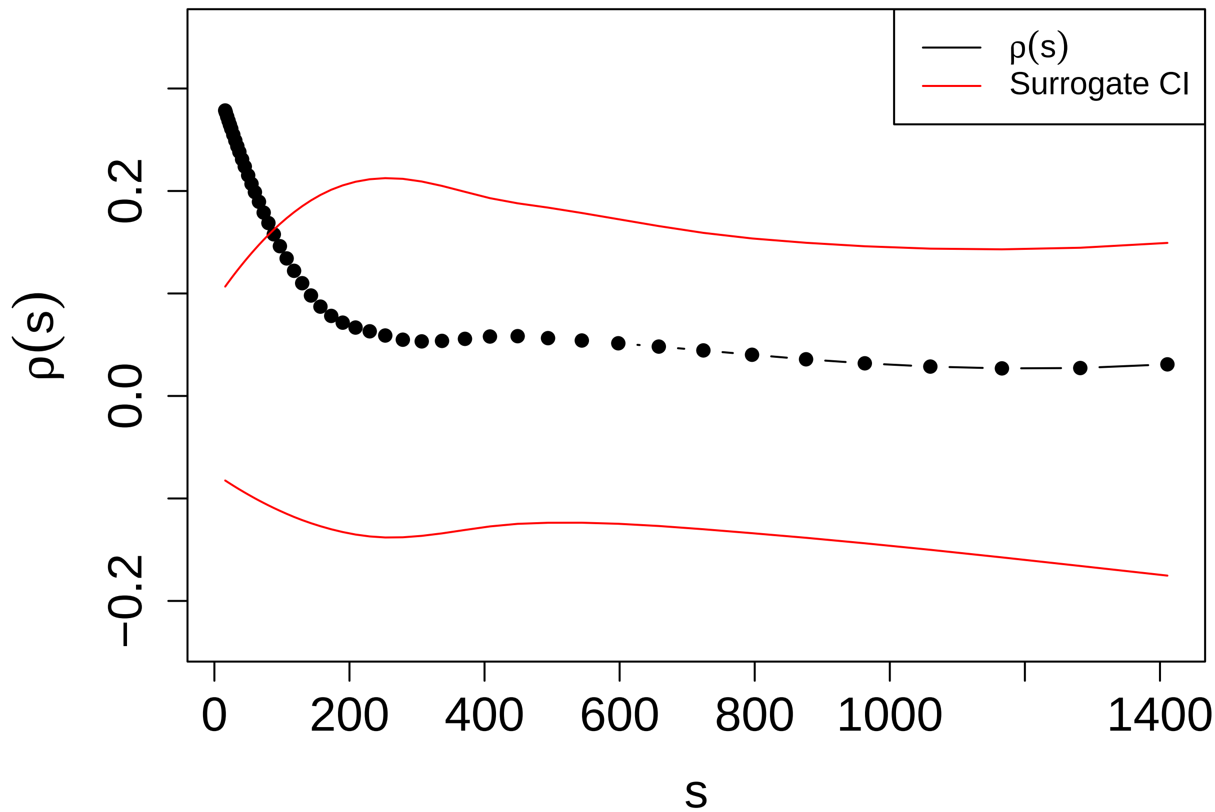

In examining the output from these analyses, Figure 11 shows a clear difference between the two conditions. First, in the firm platform example, the $\rho(s)$ values reach an order of magnitude greater than in the foam condition with the max $\rho(s) = 0.73$ compared to 0.35 for the foam condition. Second, we observe for the foam example, that the time scale of maximum correlation is 73, which is a larger time scale when compared to the foam example, which had a maximum correlation at scale 16. Third, the pattern of change in correlation across scales is slightly different. The firm example is higher overall; it starts relatively low at very small time scales before a rapid increase and then steady decrease before stabilizing at increasingly larger scales. By contrast, the foam example has relatively lower overall correlation values, the smallest scale is the highest followed by a steady decrease and then also stabilizing at larger scales. Lastly, we can also derive statistical conclusions because, in the firm condition, the two series are correlated at all scales, whereas the series are only correlated beyond chance at the smaller scales in the foam condition.

Multiscale Regression Analysis. Multiscale regression analysis (MRA) is a further generalization of DCCA that brings the analyses into a predictive, regression framework (Kristoufek, 2015b). The key questions that can be answered by it are: a) *How does the influence of one time series on another time series change as a function of scale?* and b) *What is/are the dominant (time) scale(s) of influence of one time series on another time series?* The algorithm is largely the same as DCCA, with a key difference being that instead of estimating scale-wise symmetric correlation coefficients, leveraging methods of Ordinary Least Squares (OLS) regression, asymmetric β coefficients are estimated (see Likens et al. (2019b); Kristoufek (2015b)) according to the following equation

$$\beta(s) = \frac{F_{xy}(s)}{F_x^2(s)}$$

The $\beta(s)$ equation differs from the $\rho(s)$ equation only in the denominator where $F_x^2(s)$ is the average squared residual at each scale and $F_xy(s)$ is still the scale-wise covariance.

MRA Examples. Considering the LRC and LRCC simulations used for DCCA, we can examine whether the scale-wise fluctuations of one variable can predict the scale-wise fluctuations of the other using `mra()`. As with a traditional regression approach, we will use one of our variables as our predictor (x_t) and the other as our outcome (y_t). In the example below, we again first define our logarithmically spaced scales. We then apply the `mra()` function to the two simulated time series. In this case, it's important to specify which is variable is `x` (the predictor) and which is `y` (the outcome).

We can then visualize these results as shown below in Figure 12. Generally, we observe that the β coefficients are relatively stable at increasing time scales with a general, perhaps quadratically increasing trend. Here it is also important to investigate the change in R^2 as well as the t-values. Below we see that the R^2 is quite high at most of the time scales with $R^2_{min} = 0.67$ and $R^2_{max} = 1.85$ and all $\beta(s)$ exceed the confidence intervals, implying conventional statistical significance. So between these two component ARFIMA processes, the output of MRA shows that much of the scale specific variance in y_t is explained and predicted by x_t.

Figure 12

MRA output for long range correlation and long range cross-correlation

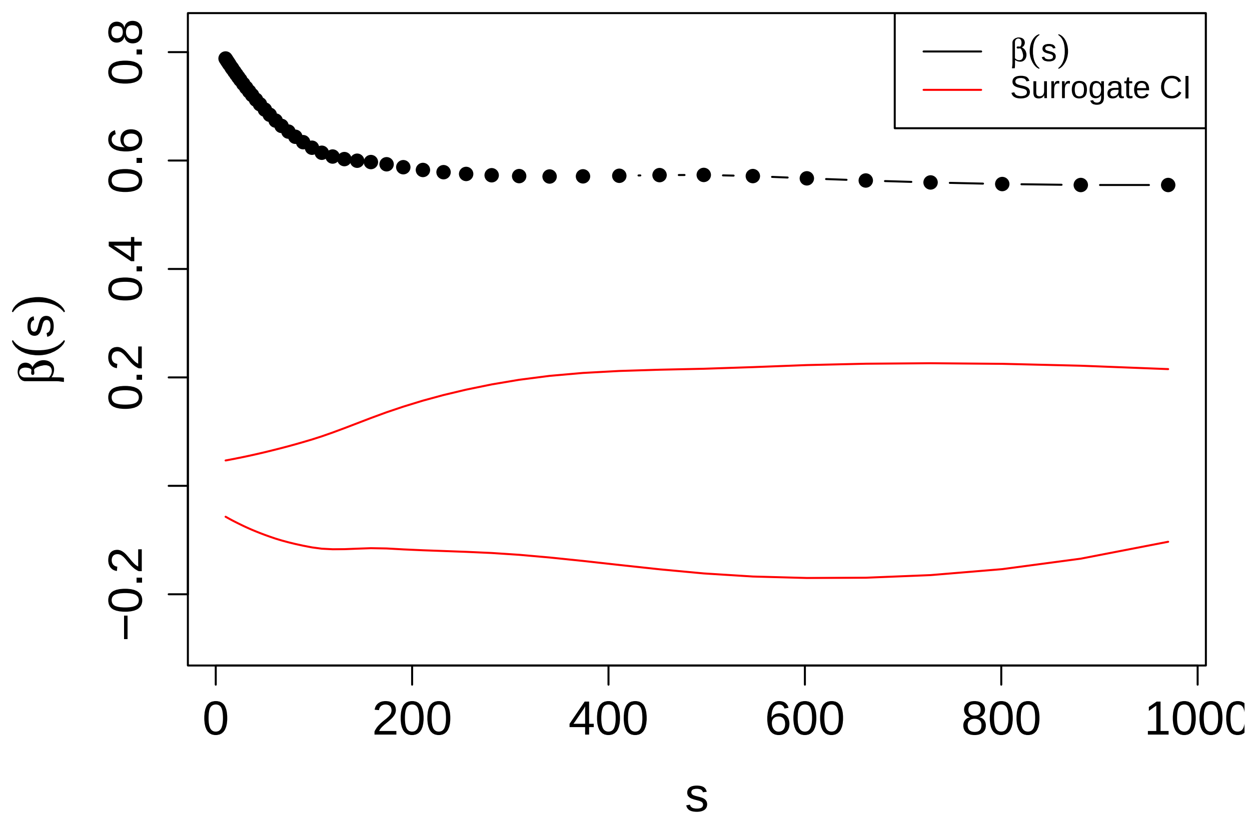

Turning next to the empirical balance data, we can determine whether postural adjustments in the COPx are predictive of adjustments in COPy, and vice versa. This means that we use the `mra()` function two times and reverse the order of entry for the x and y arguments to allow for determining the degree to which each signal can predict the other across scales. In Figure 13 below, we see the resulting β's we observed for the the balance data on the firm surface. Notably, the COPx predicting COPy (max $\beta = 0.19$) has noticeably smaller β values compared to COPy predicting COPx (max $\beta = 3.25$). Notice as well how Figure 13 (bottom), where adjustments in the y dimension are predicting adjustments in the x dimension, resembles the DCCA plot for this analysis (see Figure #). Given the asymmetry in the magnitude of the βs, this example suggests that postural adjustments in the y dimension appear to be driving changes in the x dimension. And, there is a clear time scale where this relationship is strongest at scales = 55, implying a dominant mode of coordination between mediolateral and anterioposterior control processes.

Figure 13

MRA output for balance data on foam surface with COPx predicting COPy (top) and COPy predicting COPx (bottom).

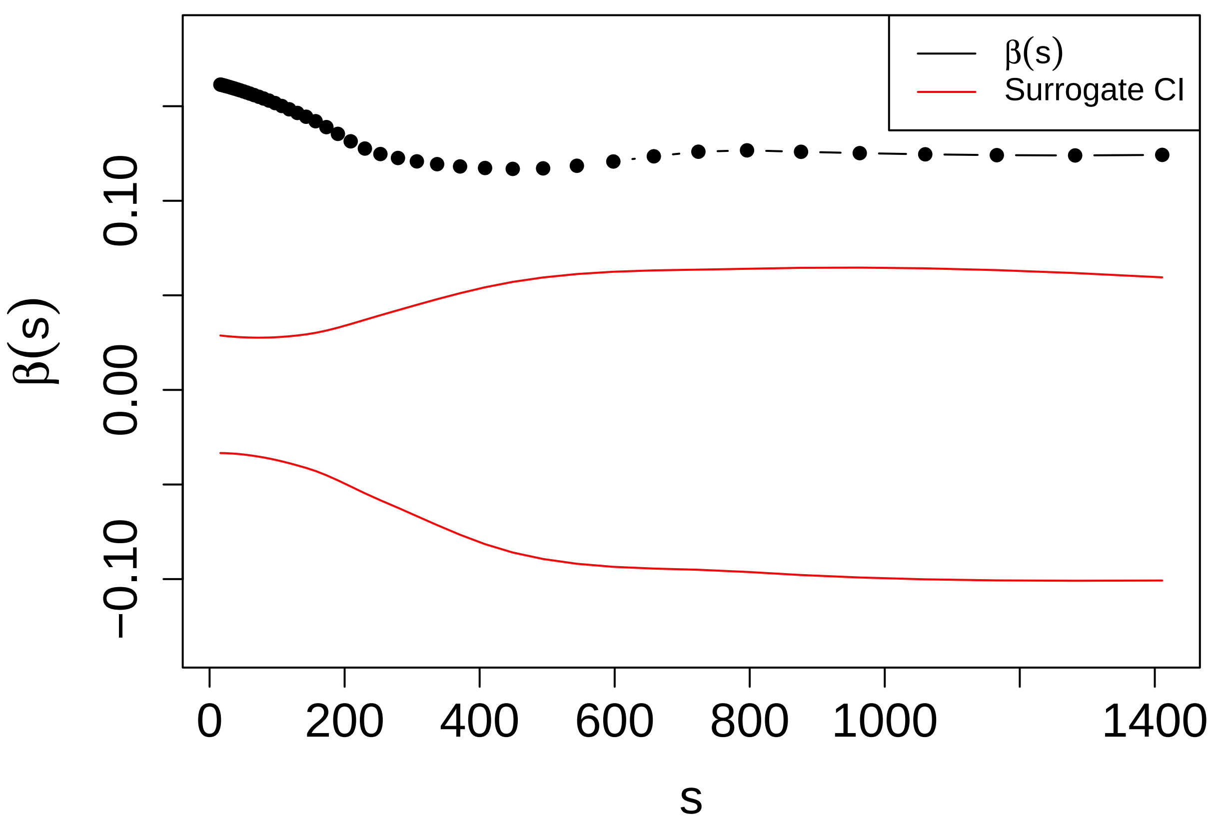

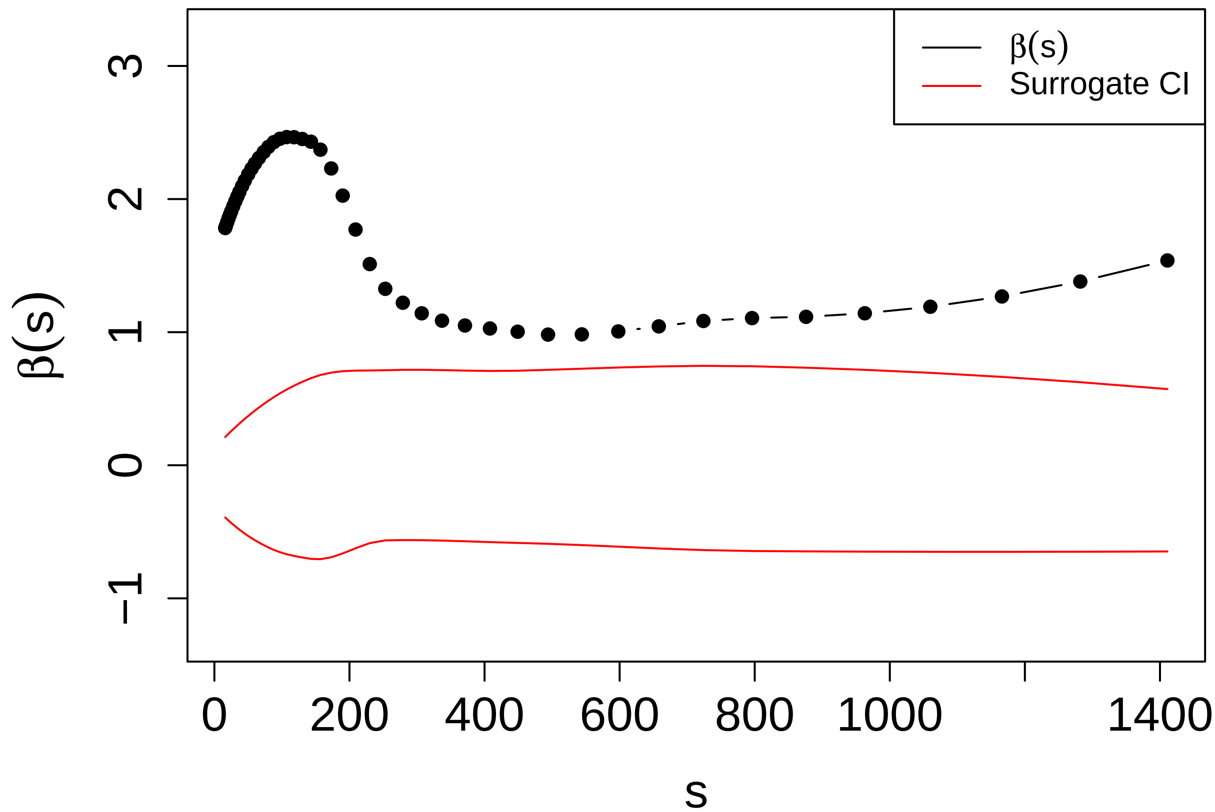

Surrogate Methods

In all of the above methods, one gets either a single estimate of a parameter (e.g., α) or a range of estimates (e.g., $\rho(s)$, $\beta(s)$). While those estimates are meaningful in and of themselves, it is common practice to perform some form of null hypothesis test regarding the estimate(s). These are generally referred to as surrogate methods Kantz and Schreiber (2003) . We present several options here that could be ranked in terms of increasing levels of rigor: randomized surrogates, iterative amplitude adjusted Fourier transformed (IAAFT) surrogates, and model-based surrogates.

Randomized Surrogates. Randomized surrogates generally involve randomly shuffling the order of values of a time series. The idea is generally that the temporal structure is destroyed, yet the other features of the time series still exist (Kantelhardt et al., 2002). Note that additional options exist along these lines (see for example (Dumas, Nadel, Soussignan, Martinerie, & Garnero, 2010)). The key comparison here would be to compare the estimates extracted from a given analysis (e.g., DFA) on the observed sample of data with the estimates derived from an equally sized sample of the surrogate series (see Kantz and Schreiber (2003) Moulder, Boker, Ramseyer, and Tschacher (2018) (**wiltshire2019?**) for examples).

Randomizing the pink noise time series, which originally exhibited long range correlation ($\alpha = 0.82$), and performing DFA on it, now provides an estimate of $\alpha = 0.55$, which is consistent with a random or white noise process. These values are clearly different, however, performing inferential statistics on a sample of observed estimates compared to surrogate estimates would provide compelling evidence that the temporal dynamics suggested by the observed estimates are different than those derived from a random process.

Iterative Amplitude-Adjusted Fourier Transform Surrogates (IAAFT). The IAAFT algorithm was originally developed as a way to discern whether nonlinearity is a feasible explanation for time series patterns (Schreiber & Schmitz, 1996). More recently, it was proposed as a technique to determine if multifractal indices suggest interaction across scales (Espen A. F. Ihlen & Vereijken, 2010). Like with randomized shuffling, estimates derived from IAAFT surrogates should be also be different from the estimates derived from the empirical time series. Although in this case, the comparison is typically made between the multifractal spectra of the observed time series, and the typical spectrum derived empirically from a set of IAAFT surrogate series.

In the code below, we provide an example for generating IAAFT surrogates using the `iaafft()` function in the package. One enters the `signal`, which is the observed time series, and `N`, the number of surrogates to generate. There are a number of options here but a common number of surrogates is 19 (Kantz & Schreiber, 2003), which allows one to establish a 95% confidence limit. In practice, surrogates are generated from each observed time series, but here we illustrate the process using only a single time series: the multifractal signal used previously in the MFDFA example. Then we use the same parameters for the `mfdfa()` function, but apply it to all of the IAAFFT surrogates. Note also that surrogate analysis is 'built-in' to our plot functions within the package as well with options to return the relevant empirically derived confidence intervals.

Assuming we were using IAAFFT to compare the multifractal width (W) between the observed signal and the surrogate signals, recall that the observed width was $W_{multi} = 1.36$. Now, we can calculate the average multifractal width across all of the generated surrogates and we observe that $W_{surr} = 0.61$, which is narrower than the spectrum from the multifractal signal. In practice, there are many surrogate options (Moulder et al., 2018), but, again, inferential statistics are commonly performed to compare observed estimates to the surrogate estimates to bolster evidence of the inferred dynamics.

Model-based Surrogates. Surrogates can also be generated when a theoretical model exists that explains the data generating process for the observed time series. Well-defined mathematical models of this nature are rare in behavioral sciences, but useful because they allow for more targeted and (potentially) realistic hypothesis testing of the underlying dynamics and how they might change due to experimental constraints. We do not provide a worked out example of such processes, but readers can consult cited papers for examples of this kind Delignières et al. (2011a).

General Discussion

In this manuscript, we provide details about the first version of a new R package aimed at bringing together a number of fractal methods that we and other researchers have found useful in analyzing a range of behavioral and physiological data. Indeed, these collective methods have found utility in virtually every area of science. Despite that reach, many researchers are not aware of these methods or lack software for their implementation. This `fractalRegression` package is our effort to bridge those gaps by demonstrating each of several methods first with simulated data, followed by equivalent demonstrations with human movement data. This allows the reader to see both the 'best case' scenario as well as the idiosyncrasies that rear their heads when we transition from the pristine world of simulation to the noisiness inherent in empirical human behavioral data.

Taken together, these methods allow for examining in univariate time seriesthe magnitude and direction of long range correlation and/or how that magnitude and direction might change over time? And in bivariate cases, these methods allow for determining: how the correlation between two time series change as a function of scale and what the dominant (time) scale(s) of coordination are. Or, relatedly, how does the influence of one time series on another change as a function of scale (at different time lags) as well as determining what the dominant (time) scale(s) of influence of one time series on another time series is (and how that might change at different time lags). Thus, these methods provide general value and can answer several types of questions on many types of data. To do so effectively, requires careful and appropriate application though. We next discuss some of these considerations.

Practical considerations for univariate methods (DFA, MFDFA). We recommend a few points of consideration in conducting DFA and MFDFA. One is to be sure to evaluate whether there are cross-over points in the log scale-log fluctuation plots (Peng et al., 1994; Perakakis, Taylor, Martinez-Nieto, Revithi, & Vila, 2009). Cross-over points (or a visible change in the slope as a function of scale) indicate that a simple mono-fractal characterization does not sufficiently characterize the data. If cross-over points are evident, we recommend proceeding to estimate the two scaling regions with a piece-wise regression (as we showed for the empirical DFA example). Note however, that for the empirical MFDFA example above, we did not parse the signal for piece-wise MFDFA although some efforts have been conducted for decomposing crossovers in multifractal signals (Nagy, Mukli, Herman, & Eke, 2017).

While it is common to use only linear detrending with DFA, this is not necessarily best practice. Instead, a more rigorous approach requires inspection of trends in the data to determine if a higher order polynomial would be more appropriate for detrending. One can then compare the DFA output for different polynomial orders (Kantelhardt et al., 2001) to determine if a genuine inflection point is present or if nonlinearity in DFA and MFDFA emerges due to undressed nonlinear trends in the original series (Likens et al., 2019b).

It's also important to consider the length of the time series being analyzed. It's common practice that in order to get reliable estimates of the metrics that minimum length of the time series is at least 512 observations although larger is better (Delignieres et al., 2006). If multiple time series are to be compared, then it's also important that they have matching lengths. Relatedly, general recommendations for choosing the min and max scale are a minimum scale of 10 and a maximum scale of N/4, where N is the total number of observations in the signal. See Eke et al. (2002) (Eke, Herman, Kocsis, & Kozak, 2002) and Gulich and Zunino (2014) (Gulich & Zunino, 2014) for additional considerations but also keep in mind specific research areas may also have other criteria Marmelat & Meidinger (2019).

Practical considerations for bivariate methods (DCCA, MRA). Many of the above considerations also apply in the bivariate case such as recommendations for length, scales sizes, and detrending. In particular, prior work has a shown a positive bias of linear and quadratic trends on MRA beta estimates at larger scales that could be mitigated with a larger detrending order (Likens et al., 2019b). Therefore it is also important to check the time series with both time and polynomial permutations of time as predictors. Additionally, pairs of signals should be equal length and at equally sampled time intervals.

Development Plan. The current release version of the `fractalRegression` package features the functions shown in Table 1. There are some additional functions that are either currently available and require some additional evaluation, or are forthcoming in future iterations of the package. For example, lagged versions of DCCA and MRA, known as Detrended Lagged Cross Correlation Analysis (DLCCA) or Multiscale Lagged Regression Analysis (MLRA) respectively, are forthcoming. These pose some new challenges for scientists as choosing a maximum time lag for example entails it's own considerations. This can in part be based on a theoretically motivated temporal distance in which the two processes might be related. In this case, it can also be a process of trial and error to determine the maximum lag to include in the analysis using visual inspection. Alternatively, there are other methods for determining a maximum time lag using a critical value that is dependent on time scales (Shen, 2015). Table 3 below shows our initial plan for function to include in future iterations of the package. Of course, as the package becomes more utilized new ideas and resources may be come available to build on the current functionality.

Table 3

Overview of development plan for `fractalRegression` *package*

Conclusion. In this paper, we advance the `fractalRegression` R package and provide examples of its use on simulated and empirical data. We hope that in collating these methods, and making them efficient, that they will be more accessible and systematically utilized across disciplines. There are many unanswered questions about these methods and the complex dynamics they are characterizing. Our hope is that this work inspires future efforts that not only apply these methods, but that also expand on them to further our understanding of the complexities of multiscale interactions in dynamic systems.

Appendix 1: Fundamental Equations

Here we will insert the fundamental equations for showcasing the algorithms. .

DFA

$$F_X = \sqrt{\frac{\sum_{j-1}^{T-s+1} f_X^2(s,j)}{T-s}}$$

where

$$f_X^2(s,j) = \frac{\sum_{k=j}^{j+s-1}(X_k - \widehat{X}_{k,j})}{s-1}$$

DCCA

$$F_Y = \sqrt{\frac{\sum_{j-1}^{T-s+1} f_Y^2(s,j)}{T-s}}$$

where

$$f_Y^2(s,j) = \frac{\sum_{k=j}^{j+s-1}(Y_k - \widehat{Y}_{k,j})}{s-1}$$

and the scale-wise covariance is estimated as:

$$f_{XY}^2(s,j) = \frac{\sum_{k=j}^{j+s-1}(X_k - \widehat{X}_{k,j})(Y_k - \widehat{Y}_{k,j})}{s-1}$$

which forms the basis for the scale-wise correlation coefficient estimated as:

$$\rho(s) = \frac{F_{XY}^2(s)}{F_X(s)F_Y(s)}$$

and for the multi-scale regression coefficients, we replace the denominator in the $\rho(s)$ equation with scale-wise variance of the predictor to estimate the scale-wise regression coefficient from regression Y_t on X_t as:

$$\widehat{\beta}(s) = \frac{F_{XY}^2(s)}{F_X^2(s)}$$

and where the variance of $\widehat{\beta}(s)$ is:

$$\sigma^2_{\widehat{\beta}(s)} = \frac{1}{T-2} \times \frac{F_u^2(s)}{F_Y^2(s)}$$

and the scale-wise residual variance, $\widehat{F}_u^2(s)$ is estimated by applying the DFA algorithm to all scale-wise residuals, $\widehat{u}_t(s)$ as:

$$\widehat{u}_t(s) = y_t - x_t\widehat{\beta}(s) - \overline{y_t - x_t\widehat{\beta}(s)}$$

Acknowledgments

Author AL receives support from a National Institutes of Health Center grant (P20GM109090), National Science Foundation grant, National Strategic Research Institute/Department of Defense, and the Nebraska Collaboration Initiative.

References

Bak, P., Tang, C., & Wiesenfeld, K. (1987). Self-organized criticality: An explanation of the 1/f noise. *Physical Review Letters*, *59*(4), 381–384. https://doi.org/10.1103/PhysRevLett.59.381

Bianchi, S. (2020). Fathon: A python package for a fast computation of detrendend fluctuation analysis and related algorithms. *Journal of Open Source Software*, *5*(45), 1828.

Cavanaugh, J. T., Kelty-Stephen, D. G., & Stergiou, N. (2017). *Multifractality, Interactivity, and the Adaptive Capacity of the Human Movement System: A Perspective for Advancing the Conceptual Basis of Neurologic Physical Therapy.* Retrieved from https://www.ingentaconnect.com/content/wk/npt/2017/00000041/00000004/art00007

Collins, J. J., & De Luca, C. J. (1993). Open-loop and closed-loop control of posture: A random-walk analysis of center-of-pressure trajectories. *Experimental Brain Research*, *95*(2), 308–318. https://doi.org/10.1007/BF00229788

Damouras, S., Chang, M. D., Sejdić, E., & Chau, T. (2010). An empirical examination of detrended fluctuation analysis for gait data. *Gait & Posture*, *31*(3), 336–340. https://doi.org/10.1016/j.gaitpost.2009.12.002

Davis, T. J., Brooks, T. R., & Dixon, J. A. (2016). Multi-scale interactions in interpersonal coordination. *Journal of Sport and Health Science*, *5*(1), 25–34. https://doi.org/10.1016/j.jshs.2016.01.015

Delignieres, D., Ramdani, S., Lemoine, L., Torre, K., Fortes, M., & Ninot, G. (2006). Fractal analyses for ‘short’ time series: A re-assessment of classical methods. *Journal of Mathematical Psychology*, *50*(6), 525–544. https://doi.org/10.1016/j.jmp.2006.07.004

Delignières, D., Almurad, Z. M. H., Roume, C., & Marmelat, V. (2016). Multifractal signatures of complexity matching. *Experimental Brain Research*, *234*(10), 2773–2785. https://doi.org/10.1007/s00221-016-4679-4

Delignières, D., Torre, K., & Bernard, P. L. (2011a). Interest of velocity variability and maximal velocity for characterizing center-of-pressure fluctuations. *Science & Motricité*, (74), 31–37. https://doi.org/10.1051/sm/2011107

Delignières, D., Torre, K., & Bernard, P.-L. (2011b). Transition from Persistent to Anti-Persistent Correlations in Postural Sway Indicates Velocity-Based Control. *PLOS Computational Biology*, *7*(2), e1001089. https://doi.org/10.1371/journal.pcbi.1001089

Delignières, D., Torre, K., & Lemoine, L. (2008). Fractal models for event-based and dynamical timers. *Acta Psychologica*, *127*(2), 382–397. https://doi.org/10.1016/j.actpsy.2007.07.007

Dumas, G., Nadel, J., Soussignan, R., Martinerie, J., & Garnero, L. (2010). Inter-Brain Synchronization during Social Interaction. *PLOS ONE*, *5*(8), e12166. https://doi.org/10.1371/journal.pone.0012166

Eddelbuettel, D., & Francois, R. (2011). Rcpp: Seamless R and C++ Integration. *Journal of Statistical Software*, *40*(1), 1–18. https://doi.org/10.18637/jss.v040.i08

Eddelbuettel, D., & Sanderson, C. (2014). RcppArmadillo: Accelerating R with high-performance C++ linear algebra. *Computational Statistics & Data Analysis*, *71*, 1054–1063. https://doi.org/10.1016/j.csda.2013.02.005

Eke, A., Herman, P., Kocsis, L., & Kozak, L. R. (2002). Fractal characterization of complexity in temporal physiological signals. *Physiological Measurement*, *23*(1), R1–R38. https://doi.org/10.1088/0967-3334/23/1/201

Euler, M. J., Wiltshire, T. J., Niermeyer, M. A., & Butner, J. E. (2016). Working memory performance inversely predicts spontaneous delta and theta-band scaling relations. *Brain Research*, *1637*, 22–33. https://doi.org/10.1016/j.brainres.2016.02.008

Garcia, C. A. (2020). *nonlinearTseries: Nonlinear Time Series Analysis*. Retrieved from https://CRAN.R-project.org/package=nonlinearTseries

Ge, E., & Leung, Y. (2013). Detection of crossover time scales in multifractal detrended fluctuation analysis. *Journal of Geographical Systems*, *15*(2), 115–147. https://doi.org/10.1007/s10109-012-0169-9

Goldberger, A. L., Amaral, L. A. N., Hausdorff, J. M., Ivanov, P. C., Peng, C.-K., & Stanley, H. E. (2002). Fractal dynamics in physiology: Alterations with disease and aging. *Proceedings of the National Academy of Sciences*, *99*(suppl 1), 2466–2472. https://doi.org/10.1073/pnas.012579499

Gulich, D., & Zunino, L. (2014). A criterion for the determination of optimal scaling ranges in DFA and MF-DFA. *Physica A: Statistical Mechanics and Its Applications*, *397*, 17–30. https://doi.org/10.1016/j.physa.2013.11.029

Hardstone, R., Poil, S.-S., Schiavone, G., Jansen, R., Nikulin, V. V., Mansvelder, H. D., & Linkenkaer-Hansen, K. (2012). Detrended Fluctuation Analysis: A Scale-Free View on Neuronal Oscillations. *Frontiers in Physiology*, *3*. https://doi.org/10.3389/fphys.2012.00450

Hausdorff, J. M., Purdon, P. L., Peng, C. K., Ladin, Z., Wei, J. Y., & Goldberger, A. L. (1996). Fractal dynamics of human gait: Stability of long-range correlations in stride interval fluctuations. *Journal of Applied Physiology*, *80*(5), 1448–1457. https://doi.org/10.1152/jappl.1996.80.5.1448

Ihlen, E. A. F. (2012). Introduction to Multifractal Detrended Fluctuation Analysis in Matlab. *Frontiers in Physiology*, *3*. https://doi.org/10.3389/fphys.2012.00141

Ihlen, Espen A. F., & Vereijken, B. (2010). Interaction-dominant dynamics in human cognition: Beyond 1/f? fluctuation. *Journal of Experimental Psychology: General*, *139*(3), 436–463. https://doi.org/10.1037/a0019098

Kantelhardt, J. W., Koscielny-Bunde, E., Rego, H. H. A., Havlin, S., & Bunde, A. (2001). Detecting long-range correlations with detrended fluctuation analysis.

Physica A: Statistical Mechanics and Its Applications, *295*(3), 441–454. https://doi.org/10.1016/S0378-4371(01)00144-3

Kantelhardt, J. W., Zschiegner, S. A., Koscielny-Bunde, E., Havlin, S., Bunde, A., & Stanley, H. E. (2002). Multifractal detrended fluctuation analysis of nonstationary time series. *Physica A: Statistical Mechanics and Its Applications*, *316*(1), 87–114. https://doi.org/10.1016/S0378-4371(02)01383-3

Kantz, H., & Schreiber, T. (2003). *Nonlinear Time Series Analysis*. Retrieved from /core/books/nonlinear-time-series-analysis/519783E4E8A2C3DCD4641E42765309C7

Kelty-Stephen, D. G. (2017). Threading a multifractal social psychology through within-organism coordination to within-group interactions: A tale of coordination in three acts. *Chaos, Solitons & Fractals*, *104*, 363–370. https://doi.org/10.1016/j.chaos.2017.08.037

Kelty-Stephen, D. G., Stirling, L. A., & Lipsitz, L. A. (2016). Multifractal temporal correlations in circle-tracing behaviors are associated with the executive function of rule-switching assessed by the Trail Making Test. *Psychological Assessment*, *28*(2), 171–180. https://doi.org/10.1037/pas0000177

Kristoufek, L. (2013). Mixed-correlated ARFIMA processes for power-law cross-correlations. *Physica A: Statistical Mechanics and Its Applications*, *392*(24), 6484–6493. https://doi.org/10.1016/j.physa.2013.08.041

Kristoufek, L. (2015a). Detrended fluctuation analysis as a regression framework: Estimating dependence at different scales. *Physical Review E*, *91*(2), 022802. https://doi.org/10.1103/PhysRevE.91.022802

Kristoufek, L. (2015b). Detrended fluctuation analysis as a regression framework: Estimating dependence at different scales. *Physical Review E*, *91*(2), 022802. https://doi.org/10.1103/PhysRevE.91.022802

Laib, M., Golay, J., Telesca, L., & Kanevski, M. (2018). Multifractal analysis of the time series of daily means of wind speed in complex regions. *Chaos, Solitons & Fractals*, *109*, 118–127. https://doi.org/10.1016/j.chaos.2018.02.024

Legrand, P., & Véhel, J. L. (2003). Signal and image processing with FracLab. *Thinking in Patterns: Fractals and Related Phenomena in Nature*, 321322.

Likens, A. D., Amazeen, P. G., West, S. G., & Gibbons, C. T. (2019a). Statistical properties of Multiscale Regression Analysis: Simulation and application to human postural control. *Physica A: Statistical Mechanics and Its Applications*, *532*, 121580. https://doi.org/10.1016/j.physa.2019.121580

Likens, A. D., Amazeen, P. G., West, S. G., & Gibbons, C. T. (2019b). Statistical properties of Multiscale Regression Analysis: Simulation and application to human postural control. *Physica A: Statistical Mechanics and Its Applications*, *532*, 121580. https://doi.org/10.1016/j.physa.2019.121580

Likens, A. D., Fine, J. M., Amazeen, E. L., & Amazeen, P. G. (2015). Experimental control of scaling behavior: What is not fractal? *Experimental Brain Research*, *233*(10), 2813–2821. https://doi.org/10.1007/s00221-015-4351-4

Marmelat, V., & Meidinger, R. L. (2019). Fractal analysis of gait in people with parkinson's disease: Three minutes is not enough. *Gait & Posture*. https://doi.org/10.1016/j.gaitpost.2019.02.023

Moulder, R. G., Boker, S. M., Ramseyer, F., & Tschacher, W. (2018). Determining synchrony between behavioral time series: An application of surrogate data generation for establishing falsifiable null-hypotheses. *Psychological Methods*, *23*(4), 757–773. https://doi.org/10.1037/met0000172

Nagy, Z., Mukli, P., Herman, P., & Eke, A. (2017). Decomposing multifractal crossovers. *Frontiers in Physiology*, *8*. Retrieved from https://www.frontiersin.org/articles/10.3389/fphys.2017.00533

Peng, C.-K., Buldyrev, S. V., Havlin, S., Simons, M., Stanley, H. E., & Goldberger, A. L. (1994). Mosaic organization of DNA nucleotides. *Physical Review E*, *49*(2), 1685–1689. https://doi.org/10.1103/PhysRevE.49.1685

Perakakis, P., Taylor, M., Martinez-Nieto, E., Revithi, I., & Vila, J. (2009). Breathing frequency bias in fractal analysis of heart rate variability. *Biological Psychology*, *82*(1), 82–88. https://doi.org/10.1016/j.biopsycho.2009.06.004

Podobnik, B., & Stanley, H. E. (2008). Detrended Cross-Correlation Analysis: A New Method for Analyzing Two Nonstationary Time Series. *Physical Review Letters*, *100*(8), 084102. https://doi.org/10.1103/PhysRevLett.100.084102

Roume, C., Almurad, Z. M. H., Scotti, M., Ezzina, S., Blain, H., & Delignières, D. (2018). Windowed detrended cross-correlation analysis of synchronization processes. *Physica A: Statistical Mechanics and Its Applications*, *503*, 1131–1150. https://doi.org/10.1016/j.physa.2018.08.074

Santos, D. A., & Duarte, M. (2016). A public data set of human balance evaluations. *PeerJ*, *4*, e2648. https://doi.org/10.7717/peerj.2648

Schaworonkow, N., & Voytek, B. (2021). Longitudinal changes in aperiodic and periodic activity in electrophysiological recordings in the first seven months of life. *Developmental Cognitive Neuroscience*, *47*, 100895. https://doi.org/10.1016/j.dcn.2020.100895

Schreiber, T., & Schmitz, A. (1996). Improved surrogate data for nonlinearity tests. *Physical Review Letters*, *77*(4), 635–638. https://doi.org/10.1103/PhysRevLett.77.635

Shen, C. (2015). Analysis of detrended time-lagged cross-correlation between two nonstationary time series. *Physics Letters A*, *379*(7), 680–687. https://doi.org/10.1016/j.physleta.2014.12.036

Snow, E. L., Likens, A. D., Allen, L. K., & McNamara, D. S. (2016). Taking Control: Stealth Assessment of Deterministic Behaviors Within a Game-Based System. *International Journal of Artificial Intelligence in Education*, *26*(4), 1011–1032. https://doi.org/10.1007/s40593-015-0085-5

Stephen, D. G., Boncoddo, R. A., Magnuson, J. S., & Dixon, J. A. (2009). The dynamics of insight: Mathematical discovery as a phase transition. *Memory & Cognition*, *37*(8), 1132–1149. https://doi.org/10.3758/MC.37.8.1132

Team, R. C. (2018). *R: A language and Environment for Statistical Computing.* Vienna, Austria.

Van Orden, G. C., Holden, J. G., & Turvey, M. T. (2003). Self-organization of cognitive performance. *Journal of Experimental Psychology: General*, *132*(3), 331–350. https://doi.org/10.1037/0096-3445.132.3.331

Zebende, G. F. (2011). DCCA cross-correlation coefficient: Quantifying level of cross-correlation. *Physica A: Statistical Mechanics and Its Applications*, *390*(4), 614–618. https://doi.org/10.1016/j.physa.2010.10.022

Function	Objective	Output
`dfa()`	Estimate long-range correlation in a time series	Object containing the overall α estimate and, if desired the `logScales` and `logRMS`
`mfdfa()`	Estimate the magnitude and range of long-range correlations in a time series	Object containing the log scales used for the analysis, the log fluctuation function for each scale and q, the various q-order exponents, Hq, Tau, h, and Dh. The base of *log* depends on scale construction and user input
`dcca()`	Estimates of scale-specific correlation between two time-series	Object containing the scales used for the analysis and the ρ ’`rho'` values for each scale
`mra()`	Estimates the scale specific regression coefficients for a predictor time series on and outcome time series	Object containing the scales and scale specific β estimates, R^2, and t statistics
`fgn_sim()`	Simulate univariate fractional Gaussian noise	Returns a vector of length `n` according to the specified `H` Hurst exponent

Function	Objective	Output
`mBm_mGn()`	Simulate univariate multi-fractional Brownian motion and Gaussian noise	Returns two vectors of length `N` according to the specified H_t series
`mc_ARFIMA()`	Simulate various types of bivariate correlated noise processes.	Returns two vectors of length `N` according to the specified noise `process` and parameters
`iaaft()`	Generate surrogate series using the iterative amplitude adjusted Fourier transform	Returns a vector of same length as input time series

	Est.	St.Err.	t value	CI(95%).l	CI(95%).u
slope1	1.36430	0.033533	40.686	1.29670	1.43190
slope2	0.42692	0.013663	31.246	0.39938	0.45445

Function	Next Release	Future Release
DLCCA	X	
MLRA	X	
Chabra-Jensen's Direct Estimation of Multifractal Spectra	X	
Bayesian Estimation of Hurst Exponent		X
Time Lag Optimization Function		X